


[View Journal Online](#)
[View Article Online](#)

Exploring flavone reactivity: A quantum mechanical study and TD-DFT benchmark on UV-vis spectroscopy

Manjeet Bhatia  *

QuantumSIMM, Kangra, Himachal Pradesh, 177105, India

* Corresponding author at: QuantumSIMM, Kangra, Himachal Pradesh, 177105, India.
 e-mail: manjeet.bhatia@quantumsimm.com (M. Bhatia).

RESEARCH ARTICLE



doi 10.5155/eurjchem.16.3.242-250.2666

Received: 03 February 2025

Received in revised form: 15 April 2025

Accepted: 29 June 2025

Published online: 30 September 2025

Printed: 30 September 2025

KEYWORDS

Global reactivity
 Electrophilic index
 Absorption spectra
 Natural bond orbital
 Dispersion correction
 Density functional theory

ABSTRACT

Flavones are known for their broad spectrum of pharmacological and biological activities, making them promising candidates for drug development and complementary medicine. In this study, a comprehensive analysis of the chemical reactivity, kinetic stability, and biological potential of the flavone molecule is performed using density functional theory (DFT) at the D3-B3LYP/6-311++G(d,p) level. The key molecular properties-proton affinity (PA), ionization energy (IE) and electron affinity (EA)-are calculated alongside global reactivity descriptors such as chemical potential (μ), chemical hardness (η), softness (σ), electrophilic index (ω), and electronegativity (χ). To ensure the reliability and cost-effectiveness of the chosen DFT method, a comparative analysis is performed using various functionals, including D3-B3LYP, wB97XD, M06-2X and MP2. Furthermore, time-dependent DFT (TD-DFT) calculations are performed with multiple functionals B3LYP, CAM-B3LYP, PBE0, M06-2X, LC-wHPBE and wB97XD to investigate the excited-state properties and UV-visible absorption spectra of flavone. The results indicate that CAM-B3LYP, M06-2X, and wB97XD provide the most accurate predictions for the absorption characteristics of the flavone molecule.

Cite this: *Eur. J. Chem.* 2025, 16(3), 242-250Journal website: www.eurjchem.com

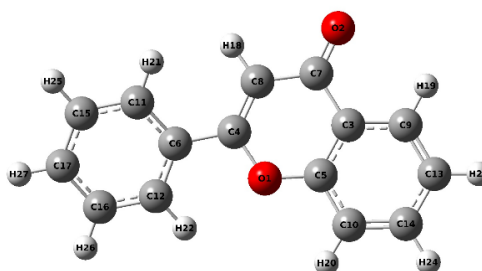
1. Introduction

Flavones are prominent among the naturally occurring compounds present in most plants and are extracted from herbs, vegetables, and fruits [1]. Flavones belong to the flavonoid class that exhibits a variety of biological activities, such as antioxidant, anti-inflammatory and anticancer effects [2,3]. They are characterized by a distinct chemical structure, consisting of a benzene ring fused to a pyrone ring. Understanding their chemical reactivity and bonding characteristics is crucial to understanding their behavior in various biological and chemical processes. Flavones are a subclass of flavonoids distinguished by a 15-carbon backbone (C6-C3-C6) that forms three rings: Ring A is a benzene ring fused to ring C. Ring C, a six-membered oxygen-containing heterocycle (a chromen-4-one ring), which includes a ketone group (C=O) and is fused with ring A. Together, rings A and C form a planar conjugated benzopyrone system. Ring B, a second benzene ring, attached at the 2-position of ring C via a single bond. The conformational flexibility of flavones arises mainly from the rotation of ring B around its single-bond connection to ring C. This rotation alters the dihedral angle between ring B and the fused A-C ring system, giving rise to different spatial forms, or conformers. In a coplanar conformer, ring B lies in the same plane as the A-C system, allowing maximum π -orbital

overlap. This extended conjugation increases the electronic delocalization of the molecule, enhancing UV absorption (important for plant pigmentation) and potentially increasing reactivity. Similarly, in a nonplanar (twisted) conformer, ring B is rotated out of the plane, which reduces conjugation but can alleviate steric hindrance, particularly when bulky groups are present. This twisted form is more likely to occur in crowded molecular environments [4]. This type of arrangement imparts unique properties to flavones, making them notable for their various biological activities and potential applications in the medicinal, nutritional, and industrial domains [5,6]. Flavones possess potent antioxidant properties [3], which help combat oxidative stress and reduce the risk of chronic diseases such as cardiovascular disorders [7] and cancer [8]. Many other potential applications of flavones include anti-inflammatory properties [4], potential in protecting neurons against oxidative damage [9] and neurodegenerative diseases such as Alzheimer [10] and Parkinson [11], and in providing nutritional value [12] to foods and may contribute to health benefits associated with plant-based diets [13]. In addition, its unique chemical structure and properties could be exploited in fields such as materials science [14], where they might contribute to the development of functional coatings [15], polymers [16], and nanomaterials [17].

Table 1. Optimized structure parameters of the flavone molecule with the D3-B3LYP/6-311++G(d,p) method. Bond lengths are in Å, and bond angles are in degrees.

| Bond | Length | Bond | Length | Bond | Angle | Bond | Angle |
|---------|--------|---------|--------|-------------|--------|-------------|--------|
| O1-C5 | 1.370 | C8-C4 | 1.355 | H19-C9-C13 | 121.92 | C9-C3-C14 | 119.91 |
| C3-C9 | 1.402 | C12-H22 | 1.081 | H20-C10-C5 | 119.33 | H24-C14-C10 | 119.42 |
| C13-H23 | 1.083 | C12-C16 | 1.391 | C7-C3-C9 | 121.71 | C5-C3-C7 | 119.72 |
| C14-C10 | 1.386 | C11-C15 | 1.389 | C4-C6-C12 | 120.12 | H18-C8-C4 | 120.09 |
| C3-C7 | 1.480 | C15-H25 | 1.083 | H27-C17-C15 | 120.12 | H26-C16-C17 | 120.09 |
| C8-H18 | 1.080 | C5-C3 | 1.397 | C11-C15-C17 | 120.24 | H21-C11-C6 | 120.02 |
| C6-C12 | 1.402 | C9-C13 | 1.403 | C11-C6-C4 | 120.73 | C11-C12-C6 | 118.95 |
| C16-H26 | 1.084 | C14-H24 | 1.084 | C5-C3-C9 | 118.57 | C7-C3-C5 | 119.72 |
| C11-H21 | 1.082 | C10-C5 | 1.395 | H23-C13-C14 | 119.87 | C5-C10-C14 | 118.78 |
| C17-H27 | 1.084 | C7-C8 | 1.454 | O1-C5-C10 | 116.52 | | |
| O1-C4 | 1.361 | C6-C4 | 1.472 | O2-C7-C8 | 123.35 | | |
| C9-H19 | 1.083 | C17-C16 | 1.393 | H22-C12-C16 | 120.19 | | |
| C13-C14 | 1.403 | C11-C6 | 1.402 | H25-C15-C11 | 119.64 | | |
| C10-H20 | 1.083 | C17-C15 | 1.394 | C17-C16-C12 | 120.27 | | |
| C7-O2 | 1.227 | | | C4-C8-C7 | 122.47 | | |

**Figure 1.** Optimized structure of the flavone molecule with D3-B3LYP/6-311++G(d,p).

Various flavonoids' structural parameters and biological activities have been extensively studied using density functional theory (DFT) calculations [18-20]. However, a detailed literature on either experimental or theoretical studies concentrated on flavone is still missing. Understanding the chemical reactivity, bonding characteristics, and kinetic stability of flavone molecules is crucial to elucidating its behavior in various chemical and biological processes. The state-of-the-art DFT-based quantum mechanical calculations are pioneered methods for revealing the electronic structure and chemical characteristics of many molecules. Global reactivity parameters such as chemical potential (μ), chemical hardness (η), softness (σ), electrophilic index (ω), and electronegativity (χ) of a molecular system offer insights into the reactivity and stability of the molecules [21,22]. The highest occupied molecular orbitals (HOMO) and the lowest unoccupied molecular orbitals (LUMO) play a decisive role in determining the chemical stability and chemical reactivity of molecular systems [21]. Proton affinity (PA), ionization energy (IE) and electron affinity (EA) are also essential to expose the proton and/or electron attachment [23]. Identifying potential electrophilic and nucleophilic sites and π -electron delocalization are crucial for elucidating chemical reactivity and various biological activities [24].

2. Experimental

DFT calculations were performed using the Gaussian 16 software package [25]. The B3LYP exchange-correlation functional [26] and the 6-311++G (d,p) basis set [27,28] were used. In molecular systems where weak interactions, such as hydrogen bonding, π - π interactions dominate, the inclusion of a dispersion correction term could provide more accurate electronic energies. This is because traditional DFT does not account for the dispersion interactions in the long-range region. The GD3-BJ is an extension of Grimme's [29] D3 dispersion correction with Becke-Johnson damping [30] to incorporate dispersion interaction effects. The dispersion correction factor induced along with the B3LYP DFT functional is critical for the

calculation of accurate electron densities. Geometry optimization, frequency calculations, and NBO analysis were performed to explore the electronic structure, reactivity, and bonding characteristics of flavone. Furthermore, electrostatic potential (ESP) analysis was conducted to interpret the charge distribution of the molecule. The DFT method, the B3LYP functional, and the 6-311++G(d,p) basis sets employed in this work are known for their accuracy in predicting electronic structure properties and provide a balance between cost and accuracy. Additionally, time-dependent DFT (TD-DFT) calculations using various functionals B3LYP, CAM-B3LYP, PBE0, M06-2X, LC-wHPBE, and wB97XD are performed to explore the excited-state properties and UV-visible absorption spectrum of the flavone molecule.

3. Results and discussion

The molecular geometry optimized from D3-B3LYP/6-311++G (d, p) DFT and basis sets combination is shown in Figure 1. The optimized molecular structure parameters (bond length and bond angles) of flavone are provided in Table 1.

From the optimized geometry, various molecular properties of the flavone molecule are computed (Table 2). These molecular properties are imperative in defining reactivity, kinetic stability, and addressing regions of potential chemical reactions. The proton affinity, dipole moment, and polarizability are computed for the investigated molecule.

The length of the bond between O2 and the proton (attached) is 0.96618 while the length of the bond between O1 and the proton is toward the higher side, that is, 0.97666. The proton affinity is computed as

$$\text{Proton affinity} = -\Delta H = -\Delta E_e - \Delta E_{ZP} + \frac{5}{2}RT \quad (1)$$

Equation 1 represents ΔE_e as the electronic energy difference between protonated and neutral molecules and ΔE_{ZP} indicates zero-point energy change of normal mode in the protonated and neutral molecule.

Table 2. Computed parameters of flavone molecule using different DFT functional with 6-311++G(d,p) basis sets. Global reactivity is obtained from the D3-B3LYP/6-311++G(d,p) method.

| Parameter | D3-B3LYP | wB97XD | M06-2X | MP2 |
|---------------------------------------|--|--|--|--|
| Proton affinity (kcal/mol) | 226.91 | 226.04 | 222.10 | - |
| Ionization energy (eV) | 8.28 | 8.57 | 8.73 | 7.17 |
| Electron affinity (eV) | 0.75 | 0.45 | 0.57 | -0.02 |
| μ_D (Debye) | 4.49 | 4.40 | 4.29 | 4.77 |
| E_{HOMO} (eV) | -6.75 | -8.68 | -8.06 | -8.98 |
| E_{LUMO} (eV) | -2.22 | -0.35 | -1.26 | 0.89 |
| ΔE_{gap} (eV) | 4.53 | 8.33 | 6.80 | 9.87 |
| E_{total} thermal (kcal/mol) | 138.15 | 139.54 | 139.46 | - |
| C_V (cal/mol K) | 50.36 | 49.72 | 49.95 | - |
| Entropy S (cal/mol K) | 112.17 | 111.48 | 111.40 | - |
| E_{vib} (kcal/mol) | 136.37 | 137.73 | 137.69 | - |
| $E_{0\ vib}$ (kcal/mol) | 130.34 | 131.78 | 131.71 | - |
| Rotational constant (GHz) | x = 1.16 y = 0.27 z = 0.22 | x = 1.17 y = 0.28 z = 0.23 | x = 1.17 y = 0.28 z = 0.23 | - |
| Dipole moment (Debye) | x = -0.3521 y = 0.2374 z = -4.4727 | x = -0.2830 y = 0.1042 z = -4.3900 | x = -0.2980 y = 0.1428 z = -4.2815 | x = -2.2661 y = -4.1758 z = 0.3797 |
| E_{total} (kcal/mol) | -138.15 | -139.50 | -139.46 | - |
| Chemical potential (μ) (eV) | -4.4855 | | | |
| Chemical hardness (η) (eV) | 2.2607 | | | |
| Softness (σ) (eV) | 0.2212 | | | |
| Electrophilic index (Ω) (eV) | 4.4499 | | | |
| Electronegativity (χ) (eV) | 4.8555 | | | |

The last term in Equation 1 represents the translational energy of the proton. Other contributions, such as ΔE_{rot} and ΔE_{vib} are neglected as compared to ΔE_{zp} (usually less than 1 kcal/mol or 4.2 KJ/mol at room temperatures, *i.e.* less than experimental error). Equations 2 and 3 denote the ionization energy and electron affinity of an N-electron atom.

$$\text{Ionization energy} = E_0(N-1) - E_0(N) \quad (2)$$

$$\text{Electron affinity} = E_0(N) - E_0(N+1) \quad (3)$$

The structural parameters derived from the D3-B3LYP method are compared with those obtained using other density functional theory (DFT) and post-Hartree-Fock correlation methods. This comparative analysis aims to provide deeper insight into how the electron correlation density influences the computed geometrical parameters. In particular, we examine results from the long-range corrected hybrid functional ω B97X-D, the high nonlocality functional M06-2X, and the second-order Møller-Plesset perturbation theory (MP2).

D3-B3LYP accounts for long-range van der Waals interactions. B3LYP is well established and widely used due to its good balance between accuracy and computational efficiency. The D3 correction improves the modeling of noncovalent interactions. While ω B97X-D, a long-range corrected hybrid functional effective for noncovalent interactions, charge-transfer complexes, and systems where long-range electron correlation is significant. On the other hand, M06-2X, a high-nonlocality hybrid meta-GGA functional with 54% Hartree-Fock exchange, designed for main group thermochemistry, kinetics and non-covalent interactions. It provides strong performance for thermochemical and kinetic properties, as well as dispersion-dominated systems provides good accuracy for a wide range of molecules. MP2, a post-Hartree-Fock method that includes electron correlation through perturbation theory up to second order more accurate than DFT for systems with moderate correlation, and provides a good benchmark for validating DFT results. MP2 is computationally expensive, especially for larger systems, and may over-correlate electrons in systems with significant static correlation. In the current study, only geometry optimization was completed, as the remaining calculations could not be performed due to high computational resource requirements.

The DFT (D3-B3LYP) computed ΔE_{gap} comply with the literature value of 4.49 Debye, -6.73, 2.28, and 4.46 eV,

respectively [31]. Sergio *et al.* reported higher values of the above quantities, however, with the CAM-B3LYP/def2TZV and HSEH1PBE/aug-cc-PVTZ theory, except for the electric dipole moment 4.42 Debye [20]. The comprehensive and reliable literature for the computed values of the structural and reactivity parameters of the flavone molecule is missing. A comparative benchmark study with range-separated hybrid functional such as ω B97XD predicts reasonably close values of PA, IE, dipole moment, and polarizability as with the B3LYP-D3(BJ) theory. However, among Minnesota functional, the M06-2X, and MP2 correlation energy values rather deviate largely from the available literature. These results show that long-range interactions can be accurately predicted via a dispersion-corrected (GD3-BJ) term combined with the B3LYP functional.

Global reactivity descriptors such as the HOMO (E_{HOMO}) and the LUMO (E_{LUMO}), energy gap ΔE_{gap} , IE, EA, and global reactivity parameters such as η , σ , χ , μ , and ω were also calculated to analyze the reactivity of the title molecule.

3.1. HOMO-LUMO

Electronic properties, including the HOMO and LUMO, were analyzed to understand the chemical reactivity and potential sites of electrophilic and nucleophilic attacks. The reactivity of a molecular system can be measured in terms of the HOMO-LUMO energy and the energy gap (ΔE_{gap}) which in turn is a measure of the excitability of the molecule. A molecule with smaller ΔE_{gap} can be easily excited compared to the molecules with larger ΔE_{gap} . The electron transfer in the proximity of lower ΔE_{gap} occurs smoothly. Bioactivity is exhibited mainly by molecules with lower ΔE_{gap} values. The larger energy gap would result in lower chemical reactivity because it is energetically unfavorable to add electrons to a high-lying LUMO or to remove electrons from a low-lying HOMO. As a result, the formation of the activated complex in any potential reaction is difficult. The schematic representation of the frontier molecular orbitals is shown in Figures 2 and 3, respectively. Molecular orbitals were visualized using GaussView software.

Frontier molecular orbitals can be expressed in terms of nucleophile and electrophile. Nucleophiles have the highest occupied molecular orbital, which interacts with the lowest unoccupied molecular orbital of the electrophile. Organic reactions occur when the HOMO of nucleophiles overlaps with the LUMO of the electrophile to form a new bond. Thus, the nucleophile can donate the electrons from the lone pair; a π -

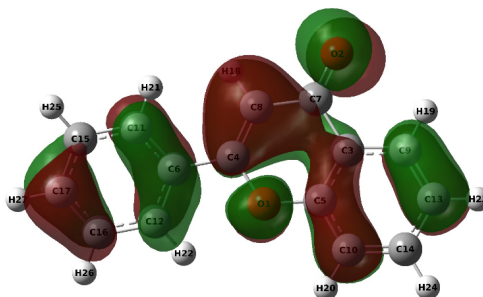


Figure 2. A pictorial representation of the HOMO of flavone molecule.

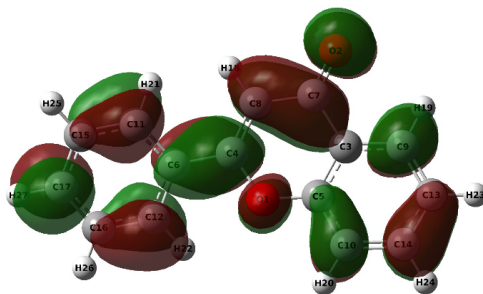


Figure 3. A pictorial representation of the LUMO of flavone molecule.

bond, or even a σ -bond, and the electrophile can accept electrons into an empty orbital or the anti-bonding orbital of a π -bond (π^* -orbital) or even the anti-bonding σ -orbital (σ^*). The antibonding orbitals have low enough energy to react if the bond is polarized by a large electronegative difference between the atoms, or even for unpolarized bonds if the bond is weak. The HOMO is primarily localized over the entire conjugated π -system of the flavone molecule, especially: the central benzopyran ring (C4-C8, C5-O1), the attached phenyl ring (C15-C17), the carbonyl oxygen (O1) and partially on C10. The red and green lobes around the aromatic carbons and O1 suggest strong π -character and non-bonding lone-pair contributions (n -orbitals) from the oxygen atom. The molecule has a high electron density on the carbonyl region and aromatic rings. The π -electrons are well delocalized, contributing to optical activity and chemical reactivity, especially in electrophilic and photochemical reactions. On the other hand, LUMO is mainly delocalized over the central benzopyran ring and partially extends toward the phenyl ring (C11-C17). The red and green lobes represent the positive and negative phases of the orbital wavefunction, respectively. These phases are key to understanding interactions in photochemical or charge-transfer processes. The LUMO indicates regions where the molecule is likely to accept electrons during excitation. Since it spans aromatic and conjugated systems, it suggests a π^* character. Mustafa and Huda [31] reported structural parameters, including a HOMO energy of -6.73 eV and a LUMO energy of -2.28 eV, using the B3LYP/6-31G basis set, which is considered a basic (weak) set. These results are in excellent agreement with the values presented in Table 2, where the HOMO energy is -6.75 eV and the LUMO energy is -2.22 eV, obtained using the D3-B3LYP level of theory.

3.2. NBO analysis

The NBO analysis reveals important intramolecular interactions, such as hydrogen bonding and hyperconjugative interactions, that influence molecular stability and reactivity. These insights aid in understanding the distribution of electron density and charge transfer within the molecule. Flavone, a

member of the flavonoid family, exhibits intriguing electron delocalization patterns within its molecular structure. Flavone is the simplest member of the class of flavones consisting of 4H-chromen-4-one bearing a phenyl substituent at position 2. It has a role as a metabolite and a nematocide. The common structure includes a C6-C3-C6 ring, which can be substituted in many ways to have a variety of subclass compounds, including flavonoids. Understanding these patterns is crucial for elucidating their reactivity and various biological activities. Electron delocalization is mainly due to the conjugation of π -electrons across its aromatic rings and oxygen atoms within the molecule. The NBO analysis suggests that all C-C bonds in flavone are characterized by sp^2 hybridized orbitals. This shows the availability of one unoccupied p -orbital. As a result, free electrons on oxygen atoms are most likely to interact with carbon orbitals through conjugation and hyperconjugation. The lone pair of O1 donates electrons to anti-bonding π -orbitals of C4 and C8, while the lone pair of O2 reveals strong interactions with C3 and C7 anti-bonding π -orbitals. The donor-acceptor interactions mentioned above are based on the highest stabilization energy as given by the second-order perturbation theory analysis of the Fock matrix (Equation 4).

$$E(2) = \Delta E_{ij} = q_i \frac{F(i,j)^2}{\epsilon_j - \epsilon_i} \quad (4)$$

where q_i is donor orbital occupancy, ϵ_i and ϵ_j are diagonal elements (orbital energies), and $F(i,j)^2$ is the off-diagonal NBO Fock matrix element. The stabilization energy $E(2)$ is associated with electron delocalization. From the NBO results, it is observed that the lone pair of O1 with the lowest occupancy and the highest energy delocalized mainly into anti-bonding π -orbitals of adjacent carbon atoms C3, C5, C4 and C8. Similarly, the O2 lone pair is delocalized on nearby anti-bonding π -orbitals of C3, C7, and C8. Studies have suggested that the ability of flavones to delocalize electrons could play a role in their anticancer properties, including their impact on cancer cell proliferation and apoptosis [20,31]. Furthermore, anti-inflammatory properties and antioxidant activity can be described in terms of its π -electron delocalization [18].

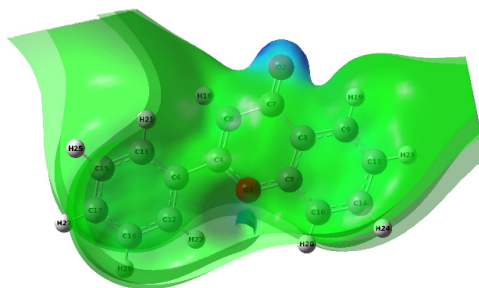


Figure 4. Electrostatic potential surface (ESP) and charge density distribution for flavone molecule.

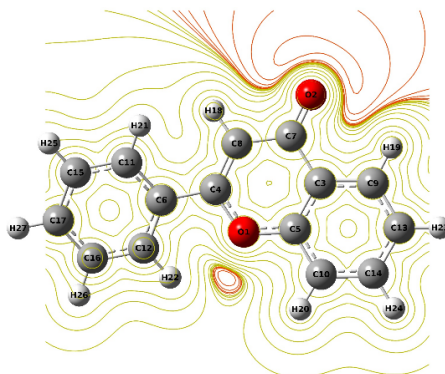


Figure 5. A contour representing the chemically active sites and comparative reactivity of atoms in a flavone molecule.

Electron delocalization in flavone contributes to its stability. Delocalized electrons are less reactive compared to localized electrons, making flavone relatively stable in its ground state. The antioxidant activity of flavones can be mapped and realized by the HOMO-LUMO orbitals, the ionization potential and the aromaticity of the structure. Previously reported results by Sergio Antonio *et al.* have shown that the flavone molecule is relatively highly aromatic [3].

3.3. Electrostatic potentials

The surface of the electrostatic potential (ESP) of the flavone molecule is shown in Figures 4 and 5. The ESP and the region of the active sites were visualized using GaussView software.

The ESP contour represents the total charge distribution (electron and nuclei) of the molecule, which determines the active sites present in a molecule. ESP analysis provides information about (i) how molecules react with each other and (ii) how to identify reactive sites in a molecule [32]. As can be seen from the PES surface diagram and contour, the flavone molecule has two potential ESP regions with higher negative charges at O1 (-0.4958) and O2 (-0.5877). The regions with negative ESP are more likely to be susceptible to electrophilic attack. However, the region with higher positive charge is more prone to nucleophilic attack. Flavone's reactivity is influenced by the distribution of electron density due to electron delocalization. The O1 and O2 atoms within flavone can act as electron-rich sites and function as nucleophiles in certain reactions, especially under basic conditions. The aromatic rings in flavone can also participate in electrophilic aromatic substitution reactions, where they act as nucleophiles by donating electrons to electrophilic species. Except for other carbon atoms with negative charges, C4, C5 and C7 atoms appear with repulsive potential with positive charges of +0.3760, +0.3373, and +0.4841, respectively. These regions of attractive and repulsive potentials appear to be most important

in determining the reactivity of flavone toward electrophilic and nucleophilic reactions.

3.4. Chemical reactivity

The global reactivity parameters of the response functions using the Koopmans approximation offer valuable insights into the behavior and reactivity of molecules and hence the overall chemistry of any molecular system. Chemical potential (μ), chemical hardness (η), softness (σ), electrophilic index (ω), and electronegativity (χ) of a molecule can be predicted from the HOMO-LUMO orbitals [33,34]. Koopman's theorem [35] approximates the ionization potential ($=-E_{\text{LUMO}}$) and the electron affinity ($=-E_{\text{HOMO}}$) with the frontier orbitals. When comparing the vertical ionization energy obtained from D3-B3LYP with that estimated using Koopman's approximation, the ionization potential is underestimated by approximately 18%. In the case of electron affinity, a direct comparison is not feasible due to significant discrepancies, with Koopman's approximation overestimating electron affinity by about 66%. On the other hand, the wB97XD method shows improved consistency. The calculated vertical ionization energy (8.57 eV) is closely aligned with the HOMO energy (8.68 eV), showing only a 1% underestimation. Furthermore, the electron affinity (0.45 eV) is slightly higher than the corresponding LUMO energy, with an overestimation of approximately 22%.

These results suggest that wB97XD offers better agreement between vertical IE and orbital energies derived from Koopman's approximation compared to D3-B3LYP. On the contrary, the M06-2X and MP2 methods perform poorly, with larger deviations observed between their vertical ionization energy values and orbital energies. Overall, wB97XD demonstrates the highest reliability among the methods tested to approximate the vertical ionization energy according to Koopman's Theorem.

Chemical reactivity descriptors can be useful in rationalizing reaction mechanisms in terms of identifying nucleophilic or electrophilic regions [22].

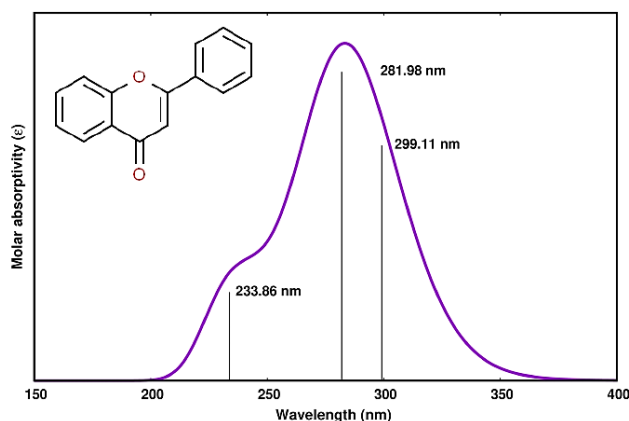


Figure 6. Absorption spectra of flavone with B3LYP/6-311++G(d,p).

The chemical potential (μ) determines the escape tendency of an electron in a molecule [24]. A higher $-\mu$ means that it is hard to lose an electron, but easier to gain. A good electrophile should have low μ values. In the context of chemical reactions, flavone can exhibit both electrophilic and nucleophilic behavior, depending on the reaction conditions and the specific functional groups present. Chemical hardness (η) and softness (σ) are obtained from the HOMO-LUMO energy gap ΔE_{gap} . A hard molecule has a large ΔE_{gap} while a soft molecule has a small ΔE_{gap} . Hard molecules are chemically less reactive but more stable, and, conversely, soft molecules are highly reactive and least stable [36]. The electrophilic index (ω) measures the ability of an electrophile to attract electrons from a nucleophile [37]. It measures the stabilization energy when the system is saturated by the electrons. For a good nucleophile, ω should be low, and for a good electrophile, ω should be higher. Similarly, electronegativity measures the tendency of an atom to strongly attract a shared pair of electrons [38]. A high χ value determines a higher ability to attract electrons [22]. These reactivity parameters are important in understanding the reactivity and stability of molecules, as they govern electron transfer processes and determine the availability of electrons for chemical reactions.

3.5. UV-vis spectroscopy benchmark

Absorption spectra and excited-state calculations are powerful tools in computational and experimental chemistry, especially when the electronic structure and photophysical properties of molecules. It helps to predict the energy levels of excited states and the transitions between them. The time-dependent DFT results for the flavone molecule are discussed in detail below.

The optimized geometry of the flavone molecule in its ground state was determined using the D3-B3LYP/6-311++G(d,p) level of theory. B3LYP is known to provide accurate predictions of the geometric structure and properties of the ground state of many organic molecules [19,39, 40,41]. B3LYP, while widely used for ground-state calculations, is known to exhibit limitations in accurately predicting excited-state properties, particularly for charge-transfer and Rydberg states. To overcome these challenges and provide a more reliable description of the electronic excitation behavior of the flavone molecule, we investigated its ultraviolet-visible (UV-vis) absorption spectrum using TD-DFT.

Several exchange-correlation functionals were employed in this analysis to evaluate their performance in modeling electronic excitations. These included CAM-B3LYP, LC- ω HPBE, M06-2X, PBE0, ω B97X-D, and the conventional B3LYP functional. Each of these functionals offers distinct advantages

in handling different aspects of electron excitation-ranging from long-range charge-transfer interactions to local excitation transitions.

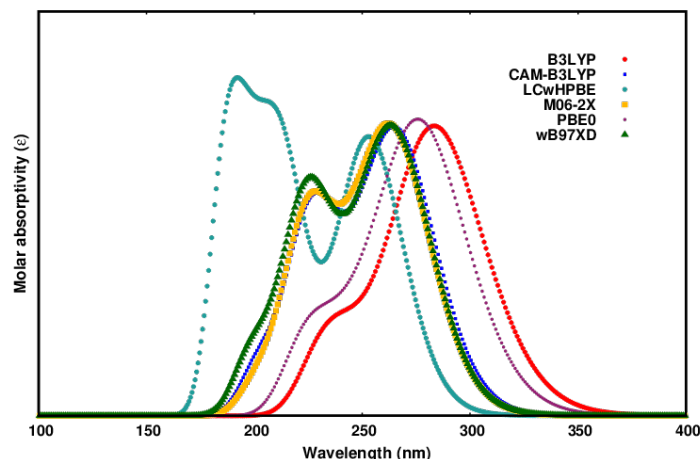
The UV-Vis spectrum was simulated by solving the time-dependent Kohn-Sham equations, as implemented in the Gaussian 16 computational chemistry software [25]. For each functional, TD-DFT calculations were carried out for the first 10 singlet excited states, enabling the identification of key absorption peaks and their corresponding transition energies and oscillator strengths. This multifunctional approach allows for a comparative assessment of the predictive accuracy of each method in reproducing the experimental/theoretical spectrum and understanding the electronic transitions in the flavone molecule.

Table 3 presents the results, including excitation energy, absorption wavelength, and oscillator strength. Flavones and flavonols typically absorb in the 240-400 nm range, generally displaying two bands: band 1 spans 300-390 nm, and band 2 covers 240-280 nm [41,42]. Specifically, flavone is characterized by absorption wavelengths of 310-350 nm in band 1 and 250-280 nm in band 2. Extensive studies on flavone absorption spectra suggest typical absorption ranges around 297 and 250 nm [43]. The absorption spectra of flavone with the B3LYP/6-311++G(d,p) DFT method are shown in Figure 6. The absorption spectra obtained using D3-B3LYP appear to be identical to those obtained with B3LYP.

Sancho *et al.* [44] conducted a spectral analysis of flavones and flavonoids in various solvents. Another benchmark study conducted by Van Bay *et al.* [45] found that the PBE0 functional is well suited for excited state calculations. The benchmark calculations in the present study suggest that CAM-B3LYP, M06-2X, and ω B97XD successfully predict the absorption bands with reasonable accuracy compared to the values of the literature. Flavone has been studied computationally with varying functionals for various properties [46]. These functionals show a high oscillator strength, with absorption bands located around 269 nm for band 2 and 223 nm for band 1. However, B3LYP places band 1 at a wavelength of 282 nm (Figure 6), while band 2 is characterized by very low intensity and the corresponding low oscillator strength, reflecting the weak intensity of band 2 (Table 3). Similarly, PBE0, which incorporates a portion of exact Hartree-Fock exchange to improve its accuracy over pure GGA functionals, fails to predict the second absorption band, as the oscillator strength and peak height are too low to be observed (Figure 7). It is noted that while CAM-B3LYP, M06-2X, and ω B97XD provide similar values, they slightly underestimate the values reported in the literature. In contrast, LC- ω HPBE, which incorporates long-range corrections to improve DFT calculations, performed poorly, predicting three absorption bands that significantly

Table 3. Shows the excited electronic state parameters computed using TD-DFT for a flavone molecule using different density functionals.

| Method | Excitation energy (eV) | Wavelength (nm) | Oscillator strength (f) |
|-----------|------------------------|-----------------|-------------------------|
| B3LYP | 4.3969 | 281.98 | 0.4166 |
| | 5.3017 | 233.86 | 0.1169 |
| CAM-B3LYP | 4.5994 | 269.57 | 0.3801 |
| | 5.4929 | 225.72 | 0.2186 |
| LC-wHPBE | 4.8643 | 254.89 | 0.4317 |
| | 5.8602 | 211.57 | 0.3439 |
| M06-2X | 6.6596 | 186.17 | 0.2614 |
| | 4.6284 | 267.88 | 0.3694 |
| PBE0 | 5.4228 | 228.64 | 0.2189 |
| | 4.5246 | 274.02 | 0.3987 |
| wB97XD | 5.5070 | 225.14 | 0.0906 |
| | 4.6331 | 267.61 | 0.3787 |
| | 5.5412 | 223.75 | 0.2513 |

**Figure 7.** Absorption spectra of flavone with different density functional.

underestimated the experimental values. Figure 7 provides a visual representation of the UV-vis spectra of flavone obtained using various density functionals. The above results confirm that CAM-B3LYP, M06-2X, and wB97XD can be well suited for excited state calculations, whereas B3LYP and PBE0 are more reliable for predicting ground state properties. As there is no definitive way to determine which functional will provide the best predictions for the molecules in question, consulting benchmark studies is the most reliable and helpful approach to begin an investigation.

Excited-state calculations reveal how stable or reactive a molecule is under light, which is crucial for designing photo-stable compounds or studying photodegradation pathways. It finds applications in drug design, materials science, especially for dyes, organic photovoltaics, and fluorescent probes, tuning absorption/emission properties is key. TD-DFT spectra are key for studying donor-acceptor systems, solar cells, and supramolecular assemblies.

4. Conclusions

In the present study, a comprehensive DFT investigation has been carried out on the flavone molecule using the D3-B3LYP/6-311++G(d,p) level of theory. This computational approach was used to analyze the chemical reactivity, kinetic stability, conformational characteristics, and bonding interactions of the molecule. The insights obtained contribute significantly to understanding the structural and electronic characteristics of flavone, which are directly linked to its biological activity and medicinal relevance.

To evaluate chemical behavior, various global reactivity descriptors were calculated, including the HOMO-LUMO energy gap, chemical potential (μ), chemical hardness (η), softness (σ), electrophilicity index (ω), and electronegativity (χ). Additional parameters such as proton affinity (PA), ionization energy (IE),

and electron affinity (EA) were also computed. The total charge distribution and reactive sites were further analyzed using natural bond orbital (NBO) and electrostatic potential (ESP) mapping.

To determine the most accurate computational method, flavone was also studied using the wB97XD, M06-2X, and MP2 methods. Among these, the D3-B3LYP method yielded results most consistent with the values in the literature for PA, IE, and the dipole moment, while MP2 exhibited the least agreement. The HOMO-LUMO energies also aligned with existing data, although previous studies used lower basis sets.

The HOMO of flavone is delocalized across the entire conjugated π -system, suggesting its involvement in electron donation during excitation. This delocalization supports flavone's photochemical activity and chemical reactivity toward electrophiles. On the contrary, the LUMO is mainly localized over the benzopyran core and extends toward the substituted phenyl ring, indicating the regions most receptive to incoming electrons.

NBO analysis revealed that lone pairs on the oxygen atoms are actively involved in donor-acceptor interactions, particularly with π^* orbitals of carbons C3, C4, C7, and C8. The orbital at carbon C7 was found to be the highest in energy, with a dominant 2py character, indicating complex electron delocalization across the structure. Oxygen atoms bear the highest negative charges, whereas carbons such as C4, C5 and C7 are highly positive, suggesting preferred sites for nucleophilic and electrophilic attacks. Furthermore, the lone pair electrons on O1 are delocalized into anti-bonding π -orbitals of C3, C4, C5 and C8, while those on O2 interact with π^* orbitals of C3, C7 and C8, reinforcing the dynamic resonance structure of the molecule. Ground-state property calculations indicate that the D3-B3LYP/6-311++G(d,p) method is the most reliable among the functionals tested. For excited-state predictions and absorption spectra, benchmark calculations

using CAM-B3LYP, M06-2X and wB97XD show that these methods are the most effective for accurately modeling flavone's optical behavior.

In general, the study highlights that the stability and chemical activity of flavones are deeply influenced by the extensive π -electron delocalization of π -electrons in its aromatic framework. These electronic features not only support their well-documented antioxidant and anti-inflammatory functions, but also offer potential in anticancer drug development, making flavone a promising molecule for continued exploration in medicinal chemistry.


Disclosure statement


Conflict of interest: The authors declare that they have no conflict of interest.
Ethical approval: All ethical guidelines have been adhered to.

ORCID and Email

Manjeet Bhatia

 manjeet.bhatia@quantumsimm.com

 manjeetbhatia83@gmail.com

 <https://orcid.org/0000-0002-6904-3549>

References

- Manach, C.; Scalbert, A.; Morand, C.; Rémésy, C.; Jiménez, L. Polyphenols: food sources and bioavailability. *The American Journal of Clinica. Nutrition* **2004**, 79 (5), 727–747.
- Donadio, G.; Mensitieri, F.; Santoro, V.; Parisi, V.; Bellone, M. L.; De Tommasi, N.; Izzo, V.; Dal Piaz, F. Interactions with Microbial Proteins Driving the Antibacterial Activity of Flavonoids. *Pharmaceutics* **2021**, 13 (5), 660.
- de Souza Farias, S. A.; da Costa, K. S.; Martins, J. B. Analysis of Conformational, Structural, Magnetic, and Electronic Properties Related to Antioxidant Activity: Revisiting Flavan, Anthocyanidin, Flavanone, Flavonol, Isoflavone, Flavone, and Flavan-3-ol. *ACS. Omega* **2021**, 6 (13), 8908–8918.
- Wang, X.; Cao, Y.; Chen, S.; Lin, J.; Bian, J.; Huang, D. Anti-Inflammation Activity of Flavones and Their Structure–Activity Relationship. *J. Agric. Food. Chem.* **2021**, 69 (26), 7285–7302.
- Addi, M.; Elbouzidi, A.; Abid, M.; Tungmunthum, D.; Elamrani, A.; Hano, C. An Overview of Bioactive Flavonoids from Citrus Fruits. *Applied Sciences* **2021**, 12 (1), 29.
- Khan, A. K.; Kousar, S.; Tungmunthum, D.; Hano, C.; Abbasi, B. H.; Anjum, S. Nano-Elicitation as an Effective and Emerging Strategy for In Vitro Production of Industrially Important Flavonoids. *Applied Sciences* **2021**, 11 (4), 1694.
- Mazidi, M.; Katsiki, N.; Banach, M. A higher flavonoid intake is associated with less likelihood of nonalcoholic fatty liver disease: results from a multiethnic study. *The Journal of Nutritional Biochemistry* **2019**, 65, 66–71.
- Zhao, L.; Yuan, X.; Wang, J.; Feng, Y.; Ji, F.; Li, Z.; Bian, J. A review on flavones targeting serine/threonine protein kinases for potential anticancer drugs. *Bioorganic & Medicinal Chemistry* **2019**, 27 (5), 677–685.
- Patel, K.; Kumar, V.; Rahman, M.; Verma, A.; Patel, D. K. New insights into the medicinal importance, physiological functions and bioanalytical aspects of an important bioactive compound of foods 'Hyperin': Health benefits of the past, the present, the future. *Beni-Suef University Journal of Basic and Applied Sciences* **2018**, 7 (1), 31–42.
- de Andrade Teles, R. B.; Diniz, T. C.; Costa Pinto, T. C.; de Oliveira Júnior, R. G.; Gama e Silva, M.; de Lavour, E. M.; Fernandes, A. W.; de Oliveira, A. P.; de Almeida Ribeiro, F. P.; da Silva, A. A.; Cavalcante, T. C.; Quintans Júnior, L. J.; da Silva Almeida, J. R. Flavonoids as Therapeutic Agents in Alzheimer's and Parkinson's Diseases: A Systematic Review of Preclinical Evidences. *Oxidative Medicine and Cellular Longevity* **2018**, 2018 (1), 7043213. <https://doi.org/10.1155/2018/7043213>.
- Meng-zhen, S.; Ju, L.; Lan-chun, Z.; Cai-feng, D.; Shu-da, Y.; Hao-fei, Y.; Wei-yan, H. Potential therapeutic use of plant flavonoids in AD and PD. *Heliyon* **2022**, 8 (11), e11440.
- Luca, S. V.; Macovei, I.; Bujor, A.; Miron, A.; Skalik-Woźniak, K.; Aprotosoaie, A. C.; Trifan, A. Bioactivity of dietary polyphenols: The role of metabolites. *Critical Reviews in Food Science and Nutrition* **2019**, 60 (4), 626–659.
- Tao, H.; Li, L.; He, Y.; Zhang, X.; Zhao, Y.; Wang, Q.; Hong, G. Flavonoids in vegetables: improvement of dietary flavonoids by metabolic engineering to promote health. *Critical Reviews in Food Science and Nutrition* **2022**, 64 (11), 3220–3234.
- Zhuang, W.; Li, Y.; Shu, X.; Pu, Y.; Wang, X.; Wang, T.; Wang, Z. The Classification, Molecular Structure and Biological Biosynthesis of Flavonoids, and Their Roles in Biotic and Abiotic Stresses. *Molecules* **2023**, 28 (8), 3599.
- Mia, R.; Toki, G. F.; Kamal, S. A. Nanoscale Coating for Flavonoid-Based Natural Colorants. *Engineering Materials* **2024**, 171–207.
- Latos-Brozio, M.; Masek, A.; Piotrowska, M. Polymeric Forms of Plant Flavonoids Obtained by Enzymatic Reactions. *Molecules* **2022**, 27 (12), 3702.
- Rizvi, M.; Gerengi, H.; Gupta, P. Functionalization of Nanomaterials: Synthesis and Characterization. *ACS. Symposium Series* **2022**, 1–26.
- Spiegel, M.; Andrúniów, T.; Sroka, Z. Flavones' and Flavonols' Antiradical Structure–Activity Relationship—A Quantum Chemical Study. *Antioxidants* **2020**, 9 (6), 461.
- Bhatti, H. A.; Uddin, N.; Ayub, K.; Saima, B.; Uroos, M.; Iqbal, J.; Anjum, S.; Light, M. E.; Hameed, A.; Khan, K. M. Synthesis, characterization of flavone, isoflavone, and 2,3-dihydrobenzofuran-3-carboxylate and density functional theory studies. *Eur. J. Chem.* **2015**, 6 (3), 305–313.
- De Souza, L. A.; Tavares, W. M.; Lopes, A. P.; Soeiro, M. M.; De Almeida, W. B. Structural analysis of flavonoids in solution through DFT 1H NMR chemical shift calculations: Epigallocatechin, Kaempferol and Quercetin. *Chemical Physics Letters* **2017**, 676, 46–52.
- Chattaraj, P. K.; Maiti, B.; Sarkar, U. Philicity: A Unified Treatment of Chemical Reactivity and Selectivity. *J. Phys. Chem. A* **2003**, 107 (25), 4973–4975.
- Jensen, F. Introduction to Computational Chemistry, 3rd ed.; John Wiley & Sons: Nashville, TN, 2016.
- Balachandran, V.; Rajeswari, S.; Lalitha, S. Vibrational spectral analysis, computation of thermodynamic functions for various temperatures and NBO analysis of 2,3,4,5-tetrachlorophenol using ab initio HF and DFT calculations. *Spectrochimica Acta Part A: Molecular and Biomolecular Spectroscopy* **2013**, 101, 356–369.
- Padmaja, L.; Ravikumar, C.; Sajan, D.; Hubert Joe, I.; Jayakumar, V. S.; Pettit, G. R.; Faurskov Nielsen, O. Density functional study on the structural conformations and intramolecular charge transfer from the vibrational spectra of the anticancer drug combretastatin-A2. *J. Raman Spectroscopy* **2008**, 40 (4), 419–428.
- Frisch, M. J.; Trucks, G. W.; Schlegel, H. B.; Scuseria, G. E.; Robb, M. A.; Cheeseman, J. R.; Montgomery, J. A.; Vreven, T.; Kudin, K. N.; Burant, J. C.; Millam, J. M.; Iyengar, S. S.; Tomasi, J.; Barone, V.; Mennucci, B.; Cossi, M.; Scalmani, G.; Rega, N.; Petersson, G. A.; Nakatsuji, H.; Hada, M.; Ehara, M.; Toyota, K.; Fukuda, R.; Hasegawa, J.; Ishida, M.; Nakajima, T.; Honda, Y.; Kitao, O.; Nakai, H.; Klene, M.; Li, X.; Knox, J. E.; Hratchian, H. P.; Cross, J. B.; Adamo, C.; Jaramillo, J.; Gomperts, R.; Stratmann, R. E.; Yazyev, O.; Austin, A. J.; Cammi, R.; Pomelli, C.; Ochterski, J. W.; Ayala, P. Y.; Morokuma, K.; Voth, G. A.; Salvador, P.; Dannenberg, J. J.; Zakrzewski, V. G.; Dapprich, S.; Daniels, A. D.; Strain, M. C.; Farkas, O.; Malick, D. K.; Rabuck, A. D.; Raghavachari, K.; Foresman, J. B.; Ortiz, J. V.; Cui, Q.; Baboul, A. G.; Clifford, S.; Cioslowski, J.; Stefanov, B. B.; Liu, G.; Liashenko, A.; Piskorz, P.; Komaromi, I.; Martin, R. L.; Fox, D. J.; Keith, T.; Al-Laham, M. A.; Peng, C. Y.; Nanayakkara, A.; Challacombe, M.; Gill, P. M. W.; Johnson, B.; Chen, W.; Wong, M. W.; Gonzalez, C.; Pople, J. A. Gaussian, Inc., Wallingford CT, 2004.
- Lee, C.; Yang, W.; Parr, R. G. Development of the Colle-Salvetti correlation-energy formula into a functional of the electron density. *Phys. Rev. B* **1988**, 37 (2), 785–789.
- Krishnan, R.; Binkley, J. S.; Seeger, R.; Pople, J. A. Self-consistent molecular orbital methods. XX. A basis set for correlated wave functions. *The Journal of Chemical Physics* **1980**, 72 (1), 650–654.
- Clark, T.; Chandrasekhar, J.; Spitznagel, G. W.; Schleyer, P. V. Efficient diffuse function-augmented basis sets for anion calculations. III. The 3-21+G basis set for first-row elements, Li–F. *J. Comput. Chem.* **1983**, 4 (3), 294–301.
- Grimme, S.; Ehrlich, S.; Goerigk, L. Effect of the Damping Function in Dispersion Corrected Density Functional Theory. *J. Comput. Chem.* **2011**, 32 (7), 1456–1465.
- Schröder, H.; Creon, A.; Schwabe, T. Reformulation of the D3(Becke–Johnson) Dispersion Correction without Resorting to Higher than C_6 Dispersion Coefficients. *J. Chem. Theory. Comput.* **2015**, 11 (7), 3163–3170.
- Mustafa, S. R.; Al-Ani, H. N. Calculation of vibrational frequencies, Energetic and some other Quantum Chemical Parameters for some Flavonoids. *J. Phys.: Conf. Ser.* **2021**, 1999 (1), 012018.
- Ali, H. M.; Ali, I. H. Structure-antioxidant activity relationships, QSAR, DFT calculation, and mechanisms of flavones and flavonols. *Med. Chem. Res.* **2019**, 28 (12), 2262–2269.
- Janak, J. F. Proof that $\Delta E_{\text{HOMO-LUMO}} = \epsilon_{\text{HOMO}} - \epsilon_{\text{LUMO}}$ in density-functional theory. *Phys. Rev. B* **1978**, 18 (12), 7165–7168.
- Parr, R. G.; Szentpály, L. v.; Liu, S. Electrophilicity Index. *J. Am. Chem. Soc.* **1999**, 121 (9), 1922–1924.

- [35]. Koopmans, T. Über die Zuordnung von Wellenfunktionen und Eigenwerten zu den Einzelnen Elektronen Eines Atoms. *Physica* **1934**, *1* (1–6), 104–113.
- [36]. Vidhya, V.; Austine, A.; Arivazhagan, M. Molecular structure, aromaticity, vibrational investigation and dual descriptor for chemical reactivity on 1- chloroisoquinoline using quantum chemical studies. *Results in Materials* **2020**, *6*, 100097.
- [37]. Chattaraj, P. K.; Sarkar, U.; Roy, D. R. Electrophilicity Index. *Chem. Rev.* **2006**, *106* (6), 2065–2091.
- [38]. Bhatia, M. An overview of conceptual-DFT based insights into global chemical reactivity of volatile sulfur compounds (VSCs). *Computational Toxicology* **2024**, *29*, 100295.
- [39]. Bhatia, M.; Manini, N.; Biasioli, F.; Cappellin, L. Calculated rate coefficients between CI-MS reagent ions and organosulfur compounds causing food taints and off-flavours. *International Journal of Mass Spectrometry* **2022**, *478*, 116860.
- [40]. Taniguchi, M.; LaRocca, C. A.; Bernat, J. D.; Lindsey, J. S. Digital Database of Absorption Spectra of Diverse Flavonoids Enables Structural Comparisons and Quantitative Evaluations. *J. Nat. Prod.* **2023**, *86* (4), 1087–1119.
- [41]. Payán-Gómez, S. A.; Flores-Holguín, N.; Pérez-Hernández, A.; Piñón-Miramontes, M.; Glossman-Mitnik, D. Computational molecular characterization of the flavonoid rutin. *Chemistry Central Journal* **2010**, *4* (1), <https://doi.org/10.1186/1752-153X-4-12>.
- [42]. Butnariu, M. Physical Properties and Identification of Flavonoids by Ultraviolet-Visible Spectroscopy. *IJBP.* **2023**, *8* (2), <https://doi.org/10.23880/ijbp-16000239>.
- [43]. Mabry, T.; Markham, K. R.; Thomas, M. B. The Systematic Identification of Flavonoids; Springer Science+Business Media: New York, NY, 2012.
- [44]. Sancho, M. I.; Almandoz, M. C.; Blanco, S. E.; Castro, E. A. Spectroscopic Study of Solvent Effects on the Electronic Absorption Spectra of Flavone and 7-Hydroxyflavone in Neat and Binary Solvent Mixtures. *IJMS.* **2011**, *12* (12), 8895–8912.
- [45]. Van Bay, M.; Hien, N. K.; Tran, P. T.; Tuyen, N. T.; Oanh, D. T.; Nam, P. C.; Quang, D. T. TD-DFT benchmark for UV-Vis spectra of coumarin derivatives. *Vietnam Journal of Chemistry* **2021**, *59* (2), 203–210.
- [46]. Sameh, A. Theoretical Study of the Hydrogenation Reactions between 1,2-diazene and Flavonoid Molecules. *Orient J. Chem.* **2012**, *28*(4), 1605–1612. <http://www.orientjchem.org/?p=11914>



Copyright © 2025 by Authors. This work is published and licensed by Atlanta Publishing House LLC, Atlanta, GA, USA. The full terms of this license are available at <https://www.eurjchem.com/index.php/eurjchem/terms> and incorporate the Creative Commons Attribution-Non Commercial (CC BY NC) (International, v4.0) License (<http://creativecommons.org/licenses/by-nc/4.0>). By accessing the work, you hereby accept the Terms. This is an open access article distributed under the terms and conditions of the CC BY NC License, which permits unrestricted non-commercial use, distribution, and reproduction in any medium, provided the original work is properly cited without any further permission from Atlanta Publishing House LLC (European Journal of Chemistry). No use, distribution, or reproduction is permitted which does not comply with these terms. Permissions for commercial use of this work beyond the scope of the License (<https://www.eurjchem.com/index.php/eurjchem/terms>) are administered by Atlanta Publishing House LLC (European Journal of Chemistry).